

SALT: Second-order Augmentation of Lattice Trusses

Michael E. McEachen[†], Thomas A. Trautt[‡] and David M. Murphy[§]
ABLE Engineering, Goleta, CA 93117

A novel structural architecture for column elements of a lattice truss has been studied and characterized, substantiating initial performance estimates. The concept substitutes a single-member truss element with a plurality of column elements, mutually braced by deployable spreaders. This new architecture produces an increase in structural hierarchy, by one order, to a second-order lattice. This general configuration has been found to be theoretically ideal for structures of the scale useful on spacecraft. The current work looks at the behavior and performance of a single column element in detail. Test article hardware was built and tested, and finite-element modeling and elasticity-theory based hand calculations were performed. The results were then extrapolated and applied to a candidate structure, the elastically stowed Coilable boom, which benefits in many ways. Primarily, the reduction in stowed strain provided by the smaller individual elements allows the use of higher specific modulus materials. The net result is roughly a 3.5X improvement in stiffness per mass, along with a reduction in stowed volume over state-of-the-art structures of equivalent strength. The increased design space, mostly towards high-strength, diameter-limited applications, brings the venerable flight-proven Coilable boom into the design regime previously accommodated only by comparatively cumbersome articulated structures.

Nomenclature

e	= eccentricity
L	= ¼ truss bay length
P	= axial load
y	= radial spread

I. Introduction

This work investigates a novel architecture: Second-order Augmentation of Lattice Trusses (SALT), specifically as applied to the helically-collapsible Coilable boom. The incorporation of an additional level of lattice hierarchy allows high specific-stiffness structural elements to be incorporated and compactly elastically stowed. The buckling strength of individual second-order column elements is improved by mutual bracing. This work looks specifically at optimizing designs that utilize unidirectional high modulus graphite composites. This type of material offers the highest stiffness-to-weight of all available structural materials, and its successful incorporation is a crucial discriminator of an optimized structure.¹ Preliminary analyses indicate that many practical SALT structures can be manufactured and packaged within the strain limits of existing continuous fiber polymer resin material systems.

The Coilable, so named for its ability to be elastically coiled into a helix for stowage, utilizes the strain energy stored within the structure to power its deployment. This eliminates the need for separate deployment actuation; a source of parasitic mass and complexity associated with other deployable systems such as articulated, inflatable and shape memory systems. Elastic stowage places a strict limit on the ratio of longeron diameter to boom diameter (stowed strain) for a given material. In a deployed truss structure, the role of a strut element is to possess sufficient stiffness in order to provide the desired natural frequency and buckling strength of the truss. Heritage structures have exclusively employed high-strain-capability glass fiber in order to allow for the largest possible longeron size for a

[†] Senior Mechanical Engineer, ABLE Engineering, 7200 Hollister Ave, Goleta, CA 93117, Member AIAA

[‡] Senior Mechanical Engineer, ABLE Engineering, 7200 Hollister Ave, Goleta, CA 93117, Member AIAA

[§] Chief Research Engineer, ABLE Engineering, 7200 Hollister Ave, Goleta, CA 93117, Member AIAA

given boom diameter. This resulted in flight structures of robust strength, but the mass performance has not yet benefited from the dramatically higher specific stiffness of modern graphite-resin systems.

Another limitation on traditional Coilables is in the scalability of structures: Coilables larger than 2 feet in diameter possess a large amount of strain energy stored in stowage that translates to a high deployment push force. To be scalable beyond this size, stowed strain energy should be sufficiently low or distributed such that no hazard exists to personnel or surrounding equipment in case of failure. This is an area in which SALT can extend the applicability of the Coilable.

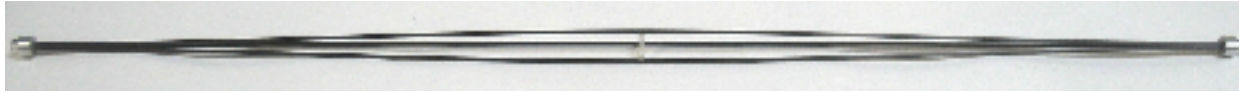


Figure 1: Embodiment of SALT

The concept of SALT is to employ multiple discrete structural elements, rods or tubes, stabilized in combination to form the elements of a global truss that act individually as columns. The constituent columns of the truss therefore essentially also become trusses. In a hierarchical structural system, this arrangement effectively increases the order of the global structure lattice by one. By doing so, deployed strength is improved for the same mass while the size of the smallest member is reduced. The resulting configuration is an extremely mass-optimized system with the high stiffness and thermal stability characteristic of high-modulus fiber composite structures.

The diagram of Figure 2 qualitatively illustrates progressive structural strength to weight efficiency for various truss column elements of equal area. By keeping the cross-sectional area of the column constant and increasing the radius of gyration, the moment of inertia- and hence the buckling strength-increases from (a) to (d). The solid rod (a) represents, nominally, the least efficient column of the series progression. The next most efficient configuration is a hollow tube, where a larger diameter improves buckling strength. In a strength-driven gossamer structure design the minimum tube wall thickness reaches a lower limit at the point of shell buckling or where practical manufacturing becomes prohibitive, as defect sensitivity cannot be mitigated. The column (c) represents the next higher evolution whereby a number of solid rods are mutually stabilized and spaced further away from the centroid, further increasing the effective column diameter. Inter-span bracing reduces the effective buckling length of the column elements to maintain local load capacity. In configuration (d) the rods are now hollow to optimize their individual performance. This pattern of hierarchical latticing can be envisioned to proceed further. However, the second order of latticing has been shown to be ideal for most space structural applications,² and thus has been investigated herein. The conceptual advancement of second order lattices for practicality as space structures is to make them deployable, as numerous SALT embodiments now allow.³

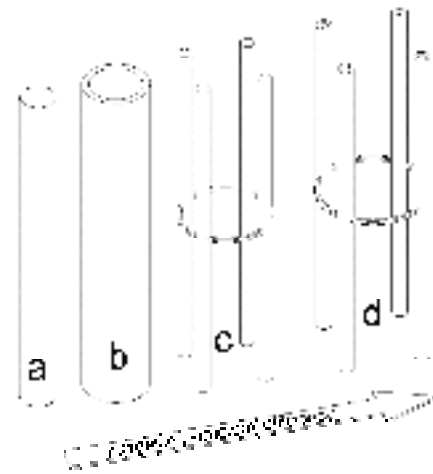


Figure 2. Structural Hierarchy

Mass efficiency is just one criteria of a useful space deployable. Another critical performance metric is stowed volume. In order to achieve packing efficiencies equal to or better than that of current elastically deployed structures, the column elements must have the ability to be consolidated in the stowed configuration and then return to the mutually braced configuration upon deployment of the system.

II. Comparison of Heritage Mast Designs with a SALT-Based Design

In order to quantify the performance improvements afforded by SALT, a comparison with a highly engineered flight system was made. In this exercise, two Coilable booms were sized to match as nearly as possible the performance of a heritage structure, the Shuttle Radar Topography Mapper (SRTM) articulated mast.⁴ The first was a typical S2 fiberglass boom with single (first-order hierarchy) solid longeron members, while the second was a SALT Coilable (second-order hierarchy) using IM9 graphite-epoxy longerons. While the S2 standard Coilable is shown here for reference, it could not have been utilized for SRTM. Its 460 lb push force would pose unacceptable personnel and facility hazard and its relatively high CTE glass fibers would be far too thermally unstable. To compare equivalent stowed-diameter assemblies, the diameter of the Coilables was increased, as the articulated SRTM boom deployment requires additional radial clearance for a deployment canister and mechanism. Coilables

may be deployed without a canister, using a rate-limiting lanyard. This allows a larger diameter boom to be stowed in the same volume. It also avoids the significant complexity, cost, and mass associated with a deployment mechanism canister, which are generally of the same magnitude as the structure itself.

The results of the boom sizing exercise are shown in Table 1. It was not possible to match the bending stiffness (EI) of the SRTM boom with a standard fiberglass Coilable boom because of the relatively low Young's Modulus of the S2 glass. The SALT boom however *does* meet this value, and at a linear mass 1/3 that of the SRTM boom. Stowed length is just over 1% of deployed length with SALT, while the SRTM boom is over 2% (over 4% when including the deployment canister and mechanism).

The ability to match or exceed, with an elastically deployed structure, the stiffness and strength of an articulated structure has many positive implications. The significant manufacturing cost associated with articulating joints, in which many complicated machined fittings are used is greatly reduced. These fittings are also subject to analysis-complicating structural nonlinearities, jitter, thermal discontinuities, and reliability concerns which are not present with continuous-longeron structures.

Table 1. Deployable Boom Sizing Comparison

Key Parameters	S2 glass	IM9 SALT	SRTM
Strain	1.75%	0.75%	n/a
Diameter	120.0	120.0	106.7 cm
Length	60	60	60 m
Slenderness	50	50	56
Pglobal	14449.6	19370.8	N
Plocal	26202.5	11863.5	N
Push Force	5857.5	757.7	n/a N
EI	1.11E+07	1.49E+07	1.48E+07 N-m ²
GJ	1.65E+04	1.65E+04	1.35E+04 N-m ²
Bending Stength	23,582	10,677	3,448 N-m
Key Dimensions			
Longeron Element Dia.	21.00	9.00	15.75 mm
Longeron Slenderness	35	81	45
Batten Dia.	14.70	8.91	15.75 mm
Diagonal Dia.	0.81	0.81	3.18 mm
Bay Length	72.8	72.8	76.2 cm
Diagonal Angle	35.0	35.0	36.0 deg
Stowed Dims			
Height	103.3	83.4	1422.4 cm
% of length	1.72	1.39	2.37 %
Mass			
Longerons	2,418.9	950.9	g/m
Battens	1,469.3	443.6	g/m
Diagonals	24.8	24.8	g/m
Balls	0.4	0.4	g/m
Fittings	179.3	154.6	g/m
Mast Total	4092.63	1574.40	4500.00 g/m

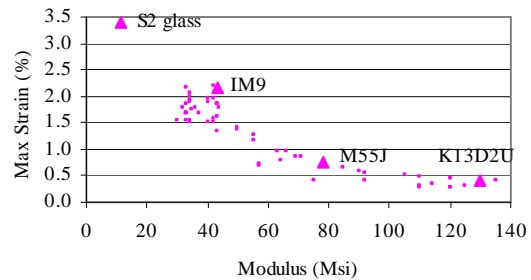
A. Material Tradeoff Discussion

The key conclusion from this comparison is that SALT technology (separation of a single element into smaller mutually-braced elements) greatly reduces the strain created by coiling the boom longerons for stowage. This enables the replacement of the heritage material for a standard Coilable (S2) with a higher specific modulus material (IM9) that provides the requisite EI at lower weight. Table 2 illustrates the performance advantage provided by graphite composites over competing materials. High modulus graphite such as M55J possesses a specific modulus

Table 2. Candidate Material Summary

	Density (lb/in ³)	Max Strain (%)	Young's Modulus (Msi)	Ultimate Strength (ksi)	Specific Modulus (MNm/kg)
Ti 6Al/4V	0.16	0.8%	15.5	127	24
Al 6061	0.098	0.4%	10.0	40	25
S2/Ep	0.073	3.4%	7.5	255	26
AlBeMet	0.076	0.1%	30.0	40	98
IM9/Ep	0.06	2.2%	27.3	920	113
M55J/Ep	0.06	0.7%	50.7	583	210

Table 3. Max Strain vs. Modulus



almost an order of magnitude higher than S-glass.

However, specific modulus is not the only consideration in fiber selection. Manufacturability and strain capability further limit material selection. Table 3 illustrates the tradeoff between modulus and strain capability for a wide variety of available fiber materials, with 4 representative fiber types labeled.

It can be seen that high strain capability cannot be obtained with the highest stiffness materials. For example, the most flexible of engineering materials, S-glass, is *one-tenth* as stiff as one of the highest-modulus fibers available (Dialead K13D2U). An excellent fiber for elastic structures is Hexcel IM9, for its compromise between strength and stiffness.⁵ Its specific stiffness is over 4 times that of S-glass.

B. Evaluation of Trends Towards Higher-Order Latticing

A study was made of columns configured as in Figure 2 (a-d) to quantitatively assess the benefits of increased lattice hierarchy on a column element in a Coilable boom. Since there is no single metric that summarizes the overall performance of a boom structure, the comparison is repeated with different metrics held fixed. This method can illuminate differences between designs that provide a relative advantage for a particular design regime. For example, a structure may possess high strength yet low stiffness, or may have such a limited design range that it is not suitable for real applications. Comparing the various configurations within the context of a Coilable boom ensures that the restrictions on material strain are realistic, and ensures that the comparison is fair. Also, for all of the comparisons, the boom diameter is held constant.

The first comparison in Table 4, seeks to minimize material mass while maintaining a nominal level of strength, equal to that provided by a standard graphite Coilable. Such a boom is mainly applicable to gossamer applications such as solar sails which are very sensitive to mass but do not require high strength. This is an example in which added hierarchy is only a slight benefit. The 28% mass reduction achieved with SALT rods is due to the

Table 4. Minimum Mass, Nominal Strength

Column Type	Solid Rod	Tube	SALT Rods	SALT Tubes
Normalized Strength	1.0	1.0	1.0	1.0
Normalized Stiffness	1.0	0.6	0.9	0.5
Normalized Mass	1.0	0.6	0.7	0.4
	Baseline for comparison	Reduced mass but also stiffness	Nearly equal stiffness w/ 30% mass reduction	Comparison w/ single tube: same stiffness, 30% mass reduction

Table 5. Maximum Strength (Normalized to S2)

Column Type	Solid Rod	Tube	SALT Rods	SALT Tubes	S2 Solid
Normalized Strength	0.2	0.5	1.0	1.0	1.0
Normalized Stiffness	0.8	0.6	1.4	0.8	1.0
Normalized Mass	0.2	0.2	0.4	0.2	1.0
Push Force	0.2	0.5	0.2	0.2	1.0
	Cannot match strength	Cannot match strength	Meets strength; Slightly stiffer; 60% mass reduction	Meets strength, 80% mass reduction	Baseline for comparison

incorporation of higher specific-stiffness fibers

employed. This is possible because the individual SALT rods of each longeron are smaller in diameter than the single rod of the non-SALT boom, and thus are strained less in stowage. The SALT tubes provide a greater mass savings, but at nearly the same cost in stiffness, a tradeoff not likely to be chosen. A SALT rod Coilable design likely best serves this low-strength specification.

Table 5 summarizes the relative performance of booms sized to possess the same strength as a fiberglass (S2) Coilable. This is a “high-strength” design, and as mentioned earlier, hierarchy is helpful mainly to increase strength per mass. This may be the most dramatic illustration of the benefits provided by SALT, which, in its rod-element form provides a 40% stiffness increase and a 61% mass reduction compared to the S2 Coilable. The SALT tube design achieves a 78% mass reduction, although with a slight reduction in stiffness. Another benefit is that the deployment force of the SALT booms is about ¼ of the S2 version, greatly enhancing its manageability.

Fixing the mass of the various designs makes another potentially illustrative comparison, shown in Table 6. One observation is that the SALT rods provide an improvement in both stiffness and strength, which means that SALT may be incorporated to a standard design with no tradeoff. For a slight tradeoff in stiffness, SALT tubes provide a dramatic 4.3X increase in strength. The stiffness reduction seen with both single and SALT tubes compared to solid rod is due to the need to use lower specific modulus, higher-strength fibers to accommodate the higher stowage strain caused by having a larger diameter longeron element.

Table 6. Equal Mass

Column Type	Solid Rod	Tube	SALT Rods	SALT Tubes
Normalized Strength	1.0	2.3	1.7	4.3
Normalized Stiffness	1.0	0.7	1.2	0.9
	Baseline for comparison	Lower stiffness because higher strain, 2.3X stronger	Slightly stiffer, 70% stronger	Slight stiffness hit, huge strength increase

III. SALT Analysis

When the SALT concept was first formulated, the biggest unknowns were the strength benefit of mutual bracing between rods, and the stiffness knockdown caused by non-straightness of the deployed rods (see Figure 1). For this recent work performance projections were first based upon estimates of real-world effects produced by the SALT configuration. Then these effects were quantified by test and analysis so that they may be better understood and addressed in the evolving design space. The work performed to date brings the level of understanding to where SALT-based system-level performance estimates can be made with confidence.

A. Influences on Strength

The performance afforded by SALT is largely dependent on the lateral stabilization provided by adjacent longeron rod elements via the spreaders. It was initially assumed that the spreaders produce an effective shortening of the effective Euler length of each rod by enforcing nodes at the spreaders. This would have the effect of increasing strength by 4X with one spreader, and 16X with three spreaders as compared to the rods alone (no spreaders). It was later found that the strengthening is created by the fact that the spread column can only twist at the middle, allowing a fixed-fixed type lateral buckling of the rods (see Figure 3). The effect is a shortening of the effective length, L_e , to one-half of the column length. Since buckling strength is a function of this length squared, this produces a 4X improvement in strength over the pin-pin end condition, which is the case with no spreader.

Another assumption was that the diameter of the spreader must be at least large enough such that the column fails with individual rods buckling (“sub-local buckling”) at around the same load as the entire column buckled (“local buckling”). This assumption was supported by analysis and test, and it results in a very small spreader when the rod strength increase is 4X (and not the 16X initially expected with multiple spreaders). A small spreader is key to minimizing the geometric stiffness knockdown, as discussed below.

B. Geometric Stiffness Knockdown

In the past, much work has been done to characterize the effects of non-straightness in slender members⁶. It is well known that for slender columns in compression, there is a strong correlation between the alignment of the load with the section centroid and the effective axial stiffness and strength. This effect becomes greatly pronounced as column slenderness ratio increases. A derivation of the stiffness knockdown for a SALT column with longeron member eccentricity introduced by a central spreader is provided in a later section. The resulting stiffness knockdown for the subject column design has 90% of the stiffness of a non-eccentric column. It was also found by analysis that the spreader stiffness itself is not a crucial determinant of column stiffness. Decreasing the spreader modulus to 5 ksi only slightly reduced the column axial stiffness, as discussed further in the finite element model (FEM) section.

C. Design Considerations

A key result for this study phase is the verification of the strength improvement provided by the cross-stabilization of rods from spreaders. As importantly, the degree of axial stiffness reduction caused by the axial deviation of the rods due to spreaders is small and quantifiable.

SALT Column Component Design: This study began with the selection of appropriately sized components for a single column test article (see Figure 1). The overall length, 36 in., was selected for testing convenience. The individual rods were sized as appropriate for a boom with a diameter corresponding to the bay (column) length. The spreader was chosen to provide the global-to-local buckling ratio discussed below.

The material used for this work was commercial-grade pultruded unidirectional carbon fiber in a BIS-F Epoxy matrix. The compressive modulus is 19 Msi. This material is readily available and provides a reasonable

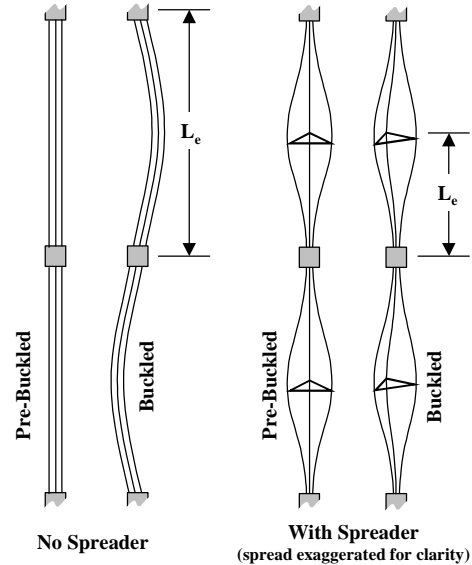


Figure 2: Spreader Effect on Buckling

approximation of the performance available with premium composites, certainly enough to indicate trends and sensitivities if not absolute performance measures.

D. Finite Element Analysis and Model

An ANSYS finite-element model of a single bay-length SALT longeron was created, as shown in Figure 4. The model was configured to have the same geometry and material properties as the prototype SALT longeron test specimen. The finite element model is composed entirely of beam elements. The spreader beams have moment releases at the ends where they intersect with the longeron rod elements. In the finite element analysis process, initially straight longeron beams laterally supported by high-CTE spreader crossbeams are “heated” to create the appropriate spread (and corresponding bowed longeron geometry) for the model. The ends are simply supported in the finite element model. Large deflection nonlinear analysis routines were used to obtain force versus deflection curves for various spreader configurations.

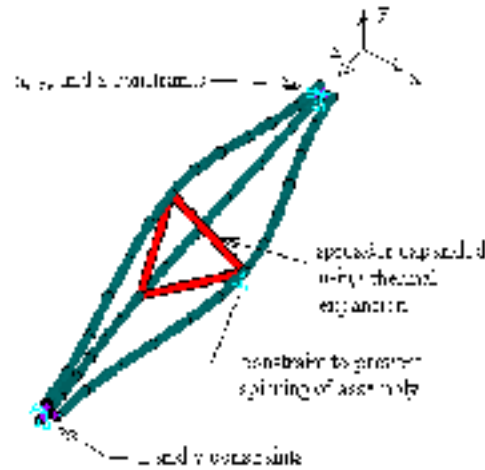


Figure 4. Finite Element Model

E. SALT Column FEM Analysis Results

Finite element results of force versus deflection and stiffness versus deflection are plotted in Figures 5 and 6, along with theoretical force and stiffness. Without waviness effects considered, as the spreader diameter increases, the initial stiffness decreases. This trend was also correlated by a closed form solution, the development of which is shown below. The longeron rods without a spreader buckle as expected for simple supports at each end. With a spreader, the longeron buckles by twisting at the spreader causing the rods to deflect out of the plane of the initial curvature and buckle as columns *with fixed ends*. Thus, the spreader increases the critical buckling load by a factor of 4, as long as the spreader diameter is large enough to produce this buckling mode.

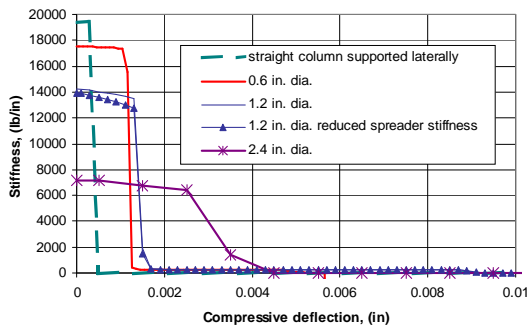


Figure 5. Force Versus Deflection Of Longeron Assemblies From Finite Element Model

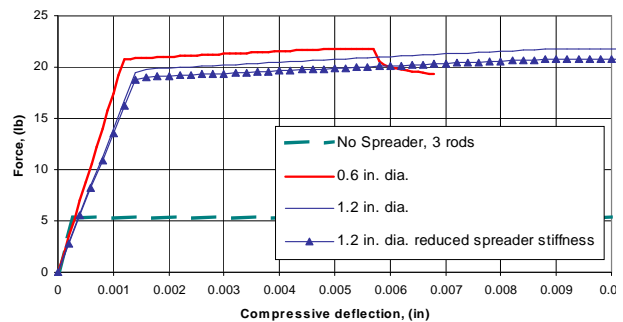


Figure 6. Stiffness Versus Deflection Of Longeron Assemblies from Finite Element Model

F. Closed-Form Analyses

Closed form (MathCAD) modeling of the SALT member stiffness performance was performed as a check on the finite element A solution for the stiffness of the SALT longeron with three rods and one spreader was derived.

G. Stiffness Derivation

The rods are assumed straight before the spreader pushes them out to a larger diameter in the middle of the longeron. The deflected rod is shown in Figure 7. Using symmetry, only a quarter of one rod needs to be analyzed. The equations are simplified because there is no moment at one end of the analyzed section.

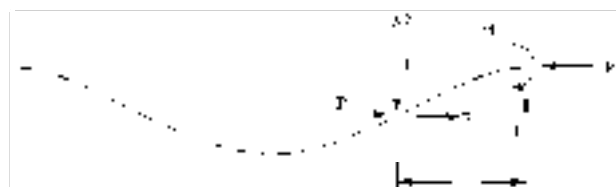


Figure 7. Deflected Rod

The following is an example solution for the SALT longeron test article configuration:

The longeron parameters are as follows:

$$\begin{aligned}
 L &:= 9 \cdot \text{in} && \text{length of 1/4 of rod} \\
 d &:= 0.125 \cdot \text{in} && \text{diameter of rod} \\
 E &:= 19 \cdot 10^6 \cdot \text{psi} && \text{Young's modulus of rod} \\
 y_0 &:= 0.14 \cdot \text{in} && \text{radial deflection at 1/4 length of the rod}
 \end{aligned}$$

The cross section properties of the rod are as follows:

$$A := \frac{\pi}{4} \cdot d^2 \quad A = 0.012 \text{ in}^2 \quad I := \frac{\pi}{64} \cdot d^4 \quad I = 1.198 \times 10^{-5} \text{ in}^4$$

The buckling strength of the longeron is calculated below.

$$P_{cr} := \frac{\pi^2 \cdot E \cdot I}{4 \cdot L^2} \quad P_{cr} = 7 \text{ lbf} \quad \text{rod buckling load} \tag{1}$$

$$P_{max} := 3 \cdot P_{cr} \quad P_{max} = 21 \text{ lbf} \quad \text{longeron buckling load} \tag{2}$$

The force versus deflection is computed below.

$$n := 100 \quad i := 0..n \quad P_i := \frac{i}{n-1} \cdot P_{cr} \quad P_n := P_{cr} \quad \gamma_i := \sqrt{\frac{P_i}{E \cdot I}} \cdot L \tag{3}$$

$$i := 1..n-1 \quad \Delta L_i := \frac{P_i \cdot L}{E \cdot A} + \frac{y_0^2 \cdot \gamma_i}{4 \cdot L} \left[\frac{\gamma_i \cdot (3 + \tan(\gamma_i)^2) - 3 \cdot \tan(\gamma_i)}{(\tan(\gamma_i) - \gamma_i)^2} \right] - \frac{3}{5} \cdot \frac{y_0^2}{L} \tag{4}$$

$$\Delta L_0 := 0 \cdot \text{in} \quad \Delta L_n := 20 \cdot \Delta L_{n-1} \tag{5}$$

$$i := 0..n \quad P_{longeron_i} := 3 \cdot P_i \quad \Delta L_{longeron_i} := 4 \cdot \Delta L_i \tag{6}$$

For comparison, the stiffness of a perfectly straight longeron is computed below.

$$k_{rod} := \frac{E \cdot A}{L} \quad k_{rod} = 25907 \frac{\text{lbf}}{\text{in}} \tag{7}$$

(¼ length of longeron)

(perfectly straight longeron)
$$k_{\text{straight}} := \frac{3 \cdot k_{\text{rod}}}{4} \quad k_{\text{straight}} = 19430 \frac{\text{lbf}}{\text{in}} \quad (8)$$

The stiffness of the longeron with the spreader with zero compressive load is computed below.

(initial stiffness of $\frac{1}{4}$ length of bent rod)
$$k_0 := \frac{k_{\text{rod}}}{1 + \frac{y_0^2}{175} \cdot \frac{A}{I}} \quad k_0 = 18970 \frac{\text{lbf}}{\text{in}} \quad (9)$$

(initial stiffness of longeron with spreader)
$$k_{\text{longeron}_0} := \frac{3}{4} \cdot k_0 \quad k_{\text{longeron}_0} = 17431 \frac{\text{lbf}}{\text{in}} \quad (10)$$

(initial stiffness of longeron with spreader)

The initial knockdown factor on stiffness:
$$\frac{k_0}{k_{\text{rod}}} = 0.897 \quad (11)$$

H. Discussion of Analysis Results

The MathCAD model and finite element models agree well, and the stiffness knockdown predicted by the use of spreaders is quite minimal. The bent shape of the rods, due to the spreaders, causes an initial stiffness reduction of only 10% versus perfectly straight rods. Manufacturing waviness in rods may introduce an additional stiffness reduction,⁷ but the effect on a SALT column will be less than for a non-SALT column because the spreaders stabilize the material at half the nominal spacing which tends to reduce the apparent waviness.

I. Eccentricity in Longerons

Some high-fidelity methods for modeling initially curved longerons in a deployed Coilable boom have been developed by ABLE under a separate program for the prediction of gossamer boom performance. Gossamer booms are susceptible to straightness deviations created by the rod manufacturing process, assembly tolerance buildup, and numerous other factors such as small bending loads coming from truss nodes (mast corner fittings). These models have application to SALT longerons where the eccentricity from straight is caused by the curves induced by spreaders.

An approximate, simplified derivation of the stiffness knockdown for a SALT column with longeron member eccentricity introduced by a central spreader is given below for comparison and crosschecking. The eccentricity, e , due to the spreader, as shown in Figure 8, is approximated by the equation 14.

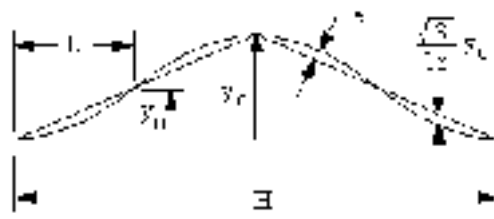


Figure 8. Eccentricity Imparted by Spreader Deployment

$$e = \frac{\sqrt{3}}{18} \cdot y_c = \frac{\sqrt{3}}{9} \cdot y_0 \quad (12)$$

A simply supported column with an initial eccentricity, e , in a half sine shape has a stiffness given by the following formula:

$$k = k_{\text{rod}} \left[1 + \frac{1}{\left(1 - \frac{P}{P_{\text{cr}}}\right)^3} \left(\frac{e^2 \cdot A}{2I} \right) \right]^{-1} \quad (13)$$

In this equation, k_{rod} is the stiffness of the straight column, 'A' is the cross section area, 'I' is the area moment of inertia, P is the applied compressive load, and P_{cr} is the critical buckling load. At zero load, the initial stiffness is:

$$k = \frac{k_{\text{rod}}}{1 + \frac{e^2 \cdot A}{2I}} \quad (14)$$

Substituting the eccentricity due to the spreader yields:

$$k = \frac{k_{\text{rod}}}{1 + \frac{y_0^2 \cdot A}{54 \cdot I}} = \frac{k_{\text{rod}}}{1 + \frac{y_c^2 \cdot A}{216 \cdot I}} \quad (15)$$

A column with fixed rotation at the ends and an initial eccentricity, e , in a cosine shape has a stiffness given by the following formula:

$$k = k_{\text{rod}} \left[1 + \frac{1}{\left(1 - \frac{P}{P_{\text{cr}}}\right)^3} \left(\frac{e^2 \cdot A}{8I} \right) \right]^{-1} \quad (16)$$

At zero load, the initial stiffness is:

$$k = \frac{k_{\text{rod}}}{1 + \frac{e^2 \cdot A}{8 \cdot I}} = \frac{k_{\text{rod}}}{1 + \frac{y_0^2 \cdot A}{216 \cdot I}} = \frac{k_{\text{rod}}}{1 + \frac{y_c^2 \cdot A}{864 \cdot I}} = 0.915 \cdot k_{\text{rod}} \quad (17)$$

Which compares well with the 0.897 factor calculated by the more rigorous derivation.

IV. Conclusions

A novel SALT architecture has been developed, which when applied to the flight heritage Coilable boom, opens up the available design space and improves performance in selected applications. By alleviating restrictions on usage of high specific stiffness material selection caused by stowage strain limitations, Coilable booms can be designed to operate in regimes previously unavailable, and with much higher mass efficiencies than provided by heritage Coilable designs. For applications similar to SRTM, high-strength applications, SALT technology has been shown to offer a 75% mass reduction for the boom alone, along with the well-known benefits of elastically deployed structures: continuous longerons without joints, an elimination of the deployment canister mechanism, and the reliability inherent to a simple structure.

This study has provided greater insight into the expected performance and handling benefits achievable by the incorporation of SALT architecture within the Coilable. Performance estimates, provided both by finite element and by closed-form calculations, encourage further development of second-order augmentation of lattice trusses, and in particular, for the Coilable boom. Construction of an engineering development boom, currently underway, will soon allow assembly-level validation of the SALT Coilable concept. Other structure types may well benefit from this architecture, and these possibilities are being studied. The mission applications considered to be the most likely candidates are large-scale, thermally and dynamically stable Synthetic Aperture Radar (SAR) structures and related stable-platform structures.

V. Acknowledgments

The work reported on herein was sponsored by NASA SBIR Phase 1 and Phase 2 contracts (NAS5 03055 and NNG04CA19C, under the technical leadership of Dr. Michael Lou of the Jet Propulsion Laboratory.

References

-
- ¹ Cadogan, D. et al., "Shape Memory Composite Development for Use in Gossamer Space Inflatable Structures," *Proceedings of the 43rd Structures, Structural Dynamics and Materials Conference*, AIAA-2002-1372, April 2002.
 - ² Murphey, T., Hinkle, J., "Some Performance Trends In Hierarchical Structures," *44th AIAA SDM Conference*, AIAA-2003-1903, 2003.
 - ³ Murphy, D. et al., Able Engineering Co., Goleta, CA, *U.S. Patent Application* 10/734,726, filed 12 Dec. 2003.
 - ⁴ Trautt, T.A., "Fly Cast Maneuver for Shuttle Radar Topography Mission," *35th Aerospace Mechanisms Symposium*, NASA/CP-2001-209626, May 2001.
 - ⁵ Hexcel Magnamite IM9 *Carbon Fiber Product Data Sheet*, March 2002.
 - ⁶ Murphy, D., "Progress and Plans for System Demonstration of a Scalable Square Solar Sail," *2004 AAS/AIAA Space Flight Mechanics Conference*, February 2004.
 - ⁷ Crawford, R.F. And Hedgepeth, J.M., "Effects of Initial Waviness on the Strength and Design of Built-up Structures," *AIAA Journal*, Vol. 13, No. 5, May 1975.